A Novel Approach for Computing Solenoidal Eigenmodes of the Vector Helmholtz Equation

Daniel A. White and Joseph M. Koning
Lawrence Livermore National Laboratory

***Abstract*—In this paper we present a novel method for computing solenoidal eigenmodes and the corresponding eigenvalues of the vector Helmholtz equation. The method employs both vector and scalar finite element basis functions to yield a discrete generalized eigenvalue problem that can be solved by standard iterative techniques. The technique is applicable for analysis of 3D inhomogeneous resonant cavities.**

I. Introduction

We are interested in determining the electromagnetic fields within closed perfectly conducting cavities that may contain dielectric and/or magnetic materials. The vector Helmholtz equation is the appropriate partial differential equation for this problem. It is well known that the electromagnetic fields in a cavity can be decomposed into distinct modes that oscillate at specific resonant frequencies. These modes are referred to as eigenmodes, and the frequencies at which these modes oscillate are referred to as eigenfrequencies. Our present application is the analysis of linear accelerator components. These components have complex geometry, hence unstructured finite-element type grids are used to model the geometry.

Numerous researchers advocate the use of $H(curl)$ vector finite elements (also know as edge, or Nedelec elements) for solving computational electromagnetics problems on unstructured grids [1]–[7]. The $H(curl)$ vector finite elements enforce the tangential continuity of fields, but allow jump discontinuities of the normal component of fields, which is required for modeling electromagnetic fields in inhomogeneous regions. In addition $H(curl)$ vector finite elements accurately model the null space of the curl operator, which has been shown to be essential for the elimination of so-called "spurious modes" in frequency domain electromagnetics [8] and charge conservation in time domain electromagnetics [9].

Electromagnetic eigenvalue problems can be solved using H(curl) vector finite elements. Typically the Galerkin procedure is used to derive a discrete form of the electric field vector Helmholtz equation, resulting in a sparse, generalized eigenvalue problem. For small problems standard dense-matrix eigenvalue algorithms such EISPACK [11] can be used to compute all of the eigenfrequencies and eigenmodes. For large problems iterative methods such as Lanczos or Arnoldi are preferred [14]. These iterative methods take advantage of the sparsity of the matrices, and in addition they allow the user to efficiently compute a small set of extremal eigenvalues (largest or smallest). In practice the user is interested in the smallest eigenvalues and the corresponding eigenmodes as these are often the dominant modes. In addition, due to the inherit discretization error of finite element methods, only the smallest eigenvalues and corresponding eigenmodes are accurate.

The difficulty in applying general-purpose iterative eigenvalue solvers towards the $H(curl)$ discretized Helmholtz equation is that this equation has a large number of zero-valued eigenvalues, corresponding to the irrotational solutions of the Helmholtz equation. This degeneracy of eigenvalues causes the iterative methods to fail to converge to the desired smallest non-zero eigenvalues. In [15] it was argued that if the initial vector used to start the Lanczos iteration were orthogonal to the null space of the curl operator than the iteration would converge to the desired solenoidal eigenmode with smallest eigenvalue. While this is true in exact arithmetic, in finite precision arithmetic this process is not numerically stable. For relatively small problems with $n \approx 1000$ even double precision is not good enough to achieve convergence. A modified Lanczos algorithm was proposed in [16] that applied a projection operator to the Lanczos vectors at every iteration to remove any irrotational components. While this method may indeed be effective for modestly sized problems, it is not clear that the method is scalable, i.e. the projection operation requires that a Poisson equation be solved to machine precision at every iteration of the Lanczos method, and this becomes increasingly difficult as the dimension of the problem increases. In [15], [17], [18] a spectral transformation is proposed such that the desired smallest non-zero eigenvalues become the extremal eigenvalues. This procedure is numerically stable and is an effective technique for achieving converge to the desired eigenvalues. In fact the authors of the ARPACK iterative eigenvalue solver package recommend this approach for

D. A. White, e-mail dwhite@llnl.gov, fax 510-423-2993.
This work was supported in part by the U.S. Department of Energy under Grant No. W-7405-Eng-48.

computing interior eigenvalues [13]. The disadvantage of this approach is that the solution of the modified eigenvalue problem requires repeated inversion of a matrix that can be quite ill-conditioned.

In this paper we present an alternative formulation of the electromagnetic eigenvalue problem in which the zero-valued eigenvalues, corresponding to the irrotational solutions of the Helmholtz equation, are arbitrarily shifted to the middle of the spectrum. Thus the desired eigenvalues are now extremal and standard iterative eigenvalue solvers can be employed without modification. The new formulation employs both $H(curl)$ vector finite elements and the standard nodal scalar finite elements. In the sections following we first review the vector Helmholtz equation and the alternative discrete formulation of the problem. Then we present results for several simple conical problems in order to validate the approach, and we finish with a real application, that of a 3D inhomogeneous linear accelerator induction cell.

II. Vector Helmholtz Equation

A. Continuous Case

We are interested in solving the vector Helmholtz equation in a 3-dimensional inhomogeneous volume Ω,

$$\nabla \times \mu^{-1} \nabla \times \vec{E} - \omega^2 \epsilon \vec{E} = 0 \; in \; \Omega, \tag{1}$$

with boundary equation $\hat{n} \times \vec{E} = 0$ on $\partial\Omega$, where $\vec{E}$ is the electric field vector, μ and ϵ are the tensor permeability and permittivity, and ω is the radian frequency. Equation (1) admits to two types of solutions; irrotational field solutions and solenoidal field solutions. An irrotational field is the gradient of a scalar potential function

$$\vec{E}_{ir} = -\nabla \phi. \tag{2}$$

Inserting (2) into (1) we see that $\omega = 0$ for irrotational fields. Conversely, by taking the divergence of (1) we see that if $\omega \neq 0$ then the field must be solenoidal,

$$\nabla \cdot \epsilon \vec{E}_s = 0. \tag{3}$$

Since the permittivity may not be continuous, equation (3) is best understood in the variational sense: we multiply (3) by a scalar potential ϕ that is zero on the boundary, and then integrate over the domain Ω and employ the divergence theorem to yield

$$\int_\Omega \epsilon \vec{E}_s \cdot \nabla \phi = 0. \tag{4}$$

Equation (4) states that a solenoidal solution of (1) is orthogonal to every irrotational field. Therefore solutions of (1) can be decomposed into irrotational ($\omega = 0$) and solenoidal ($\omega \neq 0$) solutions, with every solenoidal solution being orthogonal to every irrotational solution.

B. Discrete Case

We discretize the electric field using a $H(curl)$ finite element space $\vec{W}^h$ of dimension n defined on a mesh. We assume $H(curl)$ vector finite elements of the form proposed in [1], although the degrees of freedom can be modified (hierarchical vs. interpolatory, etc.) without any effect on the conclusions to follow. In the numerical simulations in Section V. we employ 1st-order elements; again the use of higher-order finite element basis functions does not modify premise of this paper. The discrete electric field $\tilde{E}$ is given by

$$\tilde{E} = \sum_{i=1}^{n} e_i \vec{W}_i, \tag{5}$$

where the vector $e \in \mathcal{R}^n$ is the vector of degrees-of-freedom (DOF). There is a one-to-one correspondence between $\tilde{E}$ and e. We denote the computation of $\tilde{E}$ given e as $e \rightarrow \tilde{E}$ and the computation of e given $\tilde{E}$ as $\tilde{E} \Rightarrow e$. Note that $\Rightarrow$ is a projection and can be applied to any electric field $\vec{E} \in H(curl)$, hence the computation of the approximate field $\tilde{E}$ given an arbitrary $\vec{E}$ is denoted by $\vec{E} \Rightarrow e \rightarrow \tilde{E}$.

Assume that the boundary condition $\hat{n} \times \tilde{E} = 0$ is built into the space $\vec{W}^h$. Employing the Galerkin procedure to (1) results in a generalized eigenvalue problem

$$\mathbf{A}e = \omega^2 \mathbf{B}e, \tag{6}$$

were the matrices $\mathbf{A}$ and $\mathbf{B}$ are given by

$$\mathbf{A}_{ij} = \int_\Omega \mu^{-1} \nabla \times \vec{W}_i \cdot \nabla \times \vec{W}_j, \tag{7}$$

$$\mathbf{B}_{ij} = \int_\Omega \epsilon \vec{W}_i \cdot \vec{W}_j. \tag{8}$$

The details of the computing the inner products and filling the sparse matrices can be found in finite element textbooks [19], [20] (note that the vector finite elements discussed in [20] are different the the elements used in this paper).

An important property of the $H(curl)$ vector finite element method is that the discrete Helmholtz equation (6) has the same decomposition of solutions as the original PDE. Let $L^h \subset H_1$ be the space of standard nodal finite element basis functions of dimension k defined on the interior of the mesh and of the same order as the H(curl) elements $\vec{W}^h$ (in this paper we refer to the H(curl) elements as having integer order as per [1], rather than as "half-order"). Define the subspace

$$\vec{W}^h_{ir} = \left\{ \vec{v} \in \vec{W}_h, \; \nabla \times v = 0 \right\}. \tag{9}$$

It can be shown that the finite element spaces L^h and $\vec{W}^h_{ir}$ are related by $\nabla L^h \in \vec{W}^h_{ir}$; the gradient of every nodal basis function can be written as a linear combination of

$H(curl)$ elements with zero curl [1]. This is often referred to as an inclusion condition [10], it is a discrete version of the vector identity $\nabla \times \nabla\phi = 0$. Define the vector spaces

$$F = \left\{ f \in \mathcal{R}^k, \tilde{\phi} \in L_h, \tilde{\phi} \Rightarrow f \right\} \tag{10}$$

and

$$V = \left\{ v \in \mathcal{R}^n, \tilde{E}_{ir} \in \vec{W}^h_{ir}, \tilde{E}_{ir} \Rightarrow v \right\}. \tag{11}$$

The discrete gradient operator is a sparse n by k matrix $\mathbf{P}$ such that

$$v = \mathbf{P}f, \ where \ v \in V \ and \ f \in F. \tag{12}$$

The vectors $v \in V$ form the null space of the stiffness matrix A,

$$\mathbf{AP}f = 0 \ for \ all \ f \in F. \tag{13}$$

Therefore there are exactly k solutions of (6) with $\omega = 0$, these are the static solutions of (6) with non-zero divergence.

Assume we have a discrete solenoidal solution to (6), i.e. a vector u that satisfies

$$\mathbf{A}u = \omega^2 \mathbf{B}u \ with \ \omega \neq 0. \tag{14}$$

Multiplying (14) above by an arbitrary irrotational vector $v \in V$ gives

$$v^T \mathbf{A}u = f^T \mathbf{P}^T \mathbf{A}u = \omega^2 f^T \mathbf{P}^T \mathbf{B}u = 0, \tag{15}$$

the discrete solenoidal solutions of (6) are orthogonal to the discrete irrotational solutions according to the inner product $x^T \mathbf{B} y$. Note that the product

$$f^T \mathbf{P}^T \mathbf{B}u = 0 \tag{16}$$

is exactly the discrete version of (4), the discrete solenoidal solutions u satisfy a discrete divergence-free condition. Equation (15) defines the solenoidal spaces

$$\vec{W}^h_{sol} = \left(\vec{W}^h_{ir} \right)^{\perp} \tag{17}$$

and

$$U = \left\{ u \in \mathcal{R}^n, \tilde{E}_{sol} \in \vec{W}^h_{sol}, \tilde{E}_{sol} \Rightarrow u \right\}. \tag{18}$$

In summary, we have the decompositions $\vec{W}^h = \vec{W}^h_{ir} + \vec{W}^h_{sol}$ and $\mathcal{R}^n = U + V$. The space V of dimension k is the null space of the stiffness matrix A and corresponds to irrotational solutions of (6), the space U of dimension $(n-k)$ corresponds to the solenoidal solutions. Every solution $u \in U$ is divergence-free in the sense that it satisfies (16) for all $f \in F$.

III. Iterative Methods for Eigenvalue Problems

As mentioned in the Introduction the Lanczos algorithm is a popular method for computing extremal eigenvalues of a symmetric matrix $\mathbf{A}$. The Lanczos algorithm can be applied to generalized eigenvalue problems of the form $\mathbf{A}x = \lambda \mathbf{M}x$, where $\mathbf{A}$ is symmetric and $\mathbf{M}$ is symmetric positive definite, if the inner product $< x, y >= x^T \mathbf{M} y$ is used. If the matrices $\mathbf{A}$ and $\mathbf{M}$ are not symmetric (as would result for some lossy electromagnetic media) the Arnodli algorithm is appropriate. The Arnodli algorithm reduces to the Lanczos algorithm when $\mathbf{A}$ and $\mathbf{M}$ are symmetric.

In electromagnetic applications it is a common desire to compute a small set ($m \leq 50$) of dominant eigenvalues and eigenmodes, not simply the most dominant mode. While the standard Lanczos and Arnoldi methods are efficient for computing extremal eigenvalues, the convergence towards interior eigenvalues is poor. A solution is to restart the iteration several times with new initial iterates, this is the basis for recently developed implicitly restarted Lanczos/Arnoldi methods as exemplified by the ARPACK software library [12], [13]. We propose the use of ARPACK for computing m dominant eigenvalue/eigenfrequency pairs, where m is a user specified number. To compute these eigenvalue/eigenfrequency pairs the required storage is $n \cdot O(m) + O(m^2)$ where n is the dimension of the matrices. This is significantly less storage than would be required by a standard Lanczos/Arnoldi iteration. The algorithms in ARPACK automatically restart with a new initial iterate using a sophisticate polynomial filter that enhances convergence in the direction of the desired eigenvalues. The algorithm terminates when all m eigenvalues have converged to within a user-specified tolerance. The number of restarts required for converge of all m eigenvalue is problem dependent.

Although implicitly restarted Lanczos/Arnoldi methods are superior to their non-restarted counterparts, these methods still have difficulty with our generalized eigenvalue problem (6) due to the very large number of degenerate eigenvalues at $\omega = 0$. In the next section we propose a modification of the discrete form of the vector Helmholtz equation that essentially moves the $\omega = 0$ eigenvalues towards the center of the spectrum with no effect on the solenoidal eigenvalues, and hence ARPACK can then be used without modification to compute the desired solenoidal eigenmodes and corresponding eigenfrequencies.

IV. Modified Eigenvalue Equation

First, consider Gauss' law in an inhomogeneous volume Ω

$$\nabla \cdot \epsilon \vec{E} = \rho, \tag{19}$$

where ρ is the charge density. The electric field and the scalar potential are again approximated by $\tilde{E} \in \vec{W}^h$ and $\tilde{\phi} \in L^h$, and the charge density is approximated by $\tilde{\rho} \in L^h$. Applying the Galerkin procedure yields the discrete equation

$$\mathbf{Q}e = \mathbf{N}r, \tag{20}$$

where $\tilde{E} \Rightarrow e$ and $\tilde{\rho} \Rightarrow r$, and the matrices are given by

$$\mathbf{Q}_{ij} = \int_\Omega \epsilon \vec{W}_j \cdot \nabla L_i, \tag{21}$$

$$\mathbf{N}_{ij} = \int_\Omega L_i L_j. \tag{22}$$

As discussed in Section II.B. above the matrix $\mathbf{Q} = \mathbf{P}^T\mathbf{B}$ where $\mathbf{P}$ is the discrete gradient operator that maps F to V. Clearly, from (16) the null space of $\mathbf{Q}$ is U, the space of discrete solenoidal vectors.

Using (20) above we form a generalized eigenvalue problem

$$\mathbf{Q}^T\mathbf{N}^{-1}\mathbf{Q}e = \lambda^2\mathbf{B}e. \tag{23}$$

The matrix $\mathbf{Q}^T\mathbf{N}^{-1}\mathbf{Q}$ is a square n by n matrix that can be considered to be a discretization of $\nabla\left(\nabla \cdot \epsilon\vec{E}\right)$. The eigenvalue problem (23) has the same dimensional units as our original problem (6) but does not necessary represent anything physical. It is important to note that the spectrum of (23) is exactly opposite of the spectrum of (6), i.e. equation (23) has exactly $(n-k)$ $\lambda = 0$ eigenvalues and the corresponding eigenmodes are the solenoidal vectors U, and there are exactly k eigenvalues with $\lambda > 0$ and the corresponding eigenmodes are the irrotational vectors V.

The matrix $\mathbf{Q}^T\mathbf{N}^{-1}\mathbf{Q}$ can be used to shift the irrotational eigenmodes of our orignal problem without any effect on the desired solenoidal eigenmodes. Specifically, we form the modified generalized eigenvalue problem

$$\left(\mathbf{A} + s\mathbf{Q}^T\mathbf{N}^{-1}\mathbf{Q}\right)e = \omega^2\mathbf{B}e, \tag{24}$$

where s is a user-specified parameter that shifts the irrotational eigenmodes to the middle of the spectrum. From dimensional analysis the smallest non-zero eigenvalue of (6) is approximately equal to the smallest non-zero eigenvalue of (23) therefore a shift of $s > 100$ is typically sufficient to move the spurious eigenmodes.

In Equation (24) it is not necessary to actually invert the matrix $\mathbf{N}$, it is sufficient to approximate the inverse by mass lumping. This has no effect on the desired solenoidal eigenmodes. From a purely linear algebraic point of view (24) can be written as $\mathbf{Z}e = \omega^2\mathbf{B}e$, where $\mathbf{Z}$ is a symmetric positive definite matrix. We have thus formulated the electromagnetic eigenvalue problem such that existing iterative solvers such as ARPACK can be used to compute solenoidal eigenmodes without modification.

V. Results

A. Inhomogeneous Rectangular Cavity

In order to demonstrate the efficacy of the above described algorithm we begin by analyzing the inhomogeneous cavities described in Section *A.* of [16]. These three rectangular cavities contain both a vacuum region and a dielectric region. In [16] the dominant eigenfrequency for these three cavities was computed using FDTD, a tetrahedral grid H(curl) FEM, and an analytical method, with agreement to within 0.35 percent. We modeled these cavities using a Cartesian mesh and the linear H(curl) finite elements defined in [1] along with the standard bilinear nodal finite elements. Since we are using a lower-order finite element basis function we used a mesh consisting of 15120 zones, which results is a significantly larger generalized eigenvalue problem than that in [16]. We emphasize that the purpose of this experiment is to validate the algorithm defined in Section IV. above, we are not advocating the use of lower-order finite element basis functions. We used ARPACK to compute the smallest eigenvalue of (24), and within ARPACK we used the simple Jacobi-preconditioned conjugate gradient method to "invert" the $\mathbf{B}$ matrix within every Arnoldi iteration. Our computed results agreed to the analytical results presented in [16] to within 4 decimal places.

B. Homogenous Sphere

In this section we present results for a simple homogenous sphere which has a well-known analytical solution. Although this seems like a trivial problem, it is in fact difficult due to the numerous degenerate eigenvalues. A sphere of radius $0.05855m$ was modeled using an 55296 zone unstructured mesh. This corresponds to about 36 zones per sphere radius. Linear H(curl) finite element basis functions were used, resulting generalized eigenvalue problem had $n = 162528$. In this analysis we assume the speed of light is unity. The 20 smallest eigenvalues are shown in Table I, along with the exact solution and the corresponding error.

C. Accelerator cavity

As a real application of the algorithm proposed in this paper we compute the 20 lowest eigenmodes of a linear accelerator induction cell. Of particular interest is the magnitude of the field in the accelerating gap, as this determines whether or not the particular mode will couple with the electron beam. Part of the cell is vacuum, another part consists of oil with a relative permittivity of $\epsilon = 4.5$. The induction cell was modeled using a 33024 zone unstructured hexahedral mesh, which resulted in a generalized eigenvalue problem of dimension $n = 90237$. Again, ARPACK was used to compute the 20 smallest

Mode	Exact	Computed	Percent Error
TM11	2196.39	2200.44	0.184
TM11	2196.39	2200.44	0.184
TM11	2196.39	2200.44	0.184
TM21	4368.84	4382.21	0.306
TM21	4368.84	4382.21	0.306
TM21	4368.84	4384.45	0.357
TM21	4368.84	4384.45	0.357
TM21	4368.84	4384.45	0.357
TE11	5888.69	5911.07	0.380
TE11	5888.69	5911.07	0.380
TE11	5888.69	5911.07	0.380
TM31	7214.14	7248.11	0.470
TM31	7214.14	7248.11	0.470
TM31	7214.14	7248.11	0.470
TM31	7214.14	7248.11	0.470
TM31	7214.14	7252.40	0.530
TM31	7214.14	7252.40	0.530
TM31	7214.14	7252.40	0.530
TE21	9688.19	9731.82	0.450
TE21	9688.19	9731.82	0.450

TABLE I

Exact vs. computed eigenvalues for 36 zone per radius sphere

eigenvalues of the modified generalized eigenvalue problem (24). In order to visualize the eigenmodes the magnitude of the electric field at the zone-center is computed. For example, Figures 1-4 shows the 1st, 5th, 13th, and 20th eigenmodes of the induction cell. In these illustrations only one-half of the problems is shown so that fields in the interior can be seen. Naturally, there is no analytical solution to compare to. Although it may be difficult to discern from the illustrations, the 1st and 20th modes have a maximum electric field magnitude in the accelerating gap and hence will couple strongly with the electron beam, whereas the 5th and 13th modes are examples of modes that will not couple strongly with the beam.

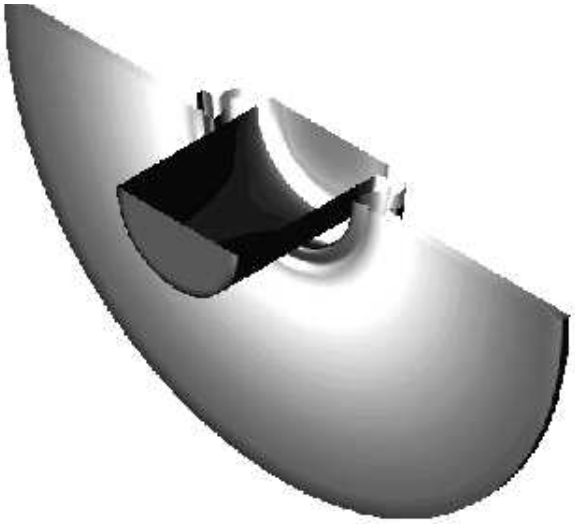

Fig. 1. 1st eigenmode of induction cell, $f = 132Mhz$

References

[1] J. C. Nedelec, "Mixed finite elements in R3," *Numer. Math.*, 35, pp. 315–341, 1980.

[2] A. Bossovit, "Whitney forms: a class of finite elements for three-dimensional computations in electromagnetism," *IEE Proceedings*, v. 135, pt. A, n. 8, pp. 493–500, 1988.

[3] A. Bossavit and I. Mayergoyz, "Edge elements for scattering problems," *IEEE Trans. Mag.*, v. 25, n. 4, pp. 2816–2821, 1989.

[4] Z. J. Cendes, "Vector finite elements for electromagnetic field problems," *IEEE Trans. Mag.*, v. 27, n. 5, pp. 3958–3966, 1991.

[5] J. F. Lee, D. K. Sun, and Z. J. Cendes, "Tangential vector finite elements for electromagnetic field computation," *IEEE Trans. Mag.*, v. 27, n. 5, pp. 4032–4035, 1991.

[6] K. Mahadevan, and R. Mittra, "Radar cross section computation of inhomogenous scatterers using edge based finite element method in time and frequency domaim," *Radio Science*, v. 28, n. 6, 1181-1193, 1993.

[7] B. Anderson and Z. Cendes, "Solution of ferrite loaded waveguide using vector finite elements," *IEEE Trans. Mag.*, v. 31, n. 3, 1578-1581, 1995.

[8] D. Sun, J. Magnes, X. Yuan, and Z. Cendes, "Spurious modes in finite element methods," *IEEE Antenna and Propagation Magazine*, v. 37, n. 5, 12-24, 1995.

[9] D. White, "Discrete time vector finite element methods for 3D unstructured grids," Ph.D. Thesis, Unviversity of California at Davis, 1993.

[10] C. Crowley, p. Solverster, and H. Hurwtiz, "Covariant projection elements for 3D vector field problems," *IEEE Trans. Mag.,* v. 24, n. 1, 397-400.

[11] B. Smith, *et. al.*, *Matrix Eigensystem Routines: EISPACK Guide*, Springer-Verlag, Berlin, 1976.

[12] R. Lehoucq, D. Sorensen, "Deflation techniques for an implcilty restarted Arnoldi method," SIAM J. Matrix Anal. Appl., v. 17, n. 4, 789-821, 1996.

[13] R. Lehoucq, D. Sorensen, C. Yang, *ARPACK User's Guide: Solution of Large-Scale Eigenvalue Problems with Implicitly Restarted Arnolid Methods*, SIAM, 1998.

[14] G. Golub and C. Van Loan, *Matrix Computations*, The Johns Hopkins University Press, Baltimore, 1989.

[15] J. Lee, D. Sun, and Z. Cendes, "Full-Wave analysis of dielectric waveguides using tangential vector finite elements," *IEEE Trans. Micro. Theor. Tech.*, v. 39, n. 8, 1262-1271, 1991.

[16] S. Perepelitsa, R. Dyczij, J. Lee, "Finite-element analysis of arbitrarily shaped cavity resonators using $H^1(curl)$ elements," *IEEE Trans. Mag.*, v. 33, n. 2, 1776-1779, 1997.

[17] J. Lee and R. Mittra, "A note on the application of edge-elements for modelling three-dimensional inhomogeneously-filled cavities," *IEEE Trans. Micro. Theor. Tech.*, v. 40, n. 9, 1767-1773, 1992.

[18] D. White and J. Koning, "Efficient solution of large scale electromagnetic eigenvalue problems using the implicitly restarted Arnoldi method," to be published in the Applied Electromagnetics Society 16th Annual Review of Progress in Computational Electromagnetics, 2000.

[19] K. Bathe, *Finite Element Procedures*, Prentice Hall, New York, 1995.

[20] J. Jin, *The Finite Element Method in Electromagnetics*, John Wiley and Sons, New York, 1993.

Fig. 2. 5th eigenmode of induction cell, $f = 280Mhz$

Fig. 3. 13th eigenmode of induction cell, $f = 439Mhz$

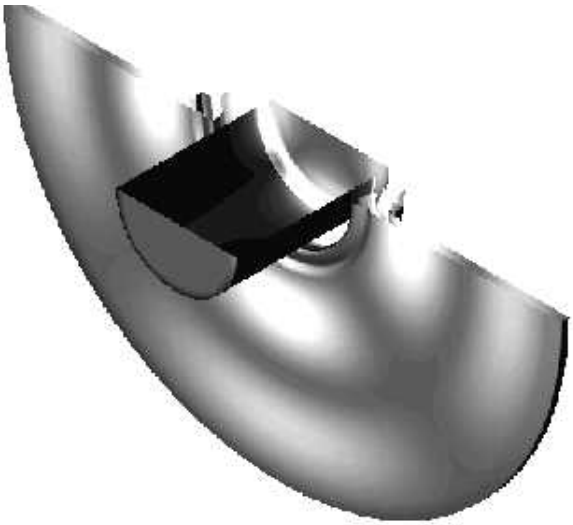

Fig. 4. 20th eigenmode of induction cell, $f = 523Mhz$